

Review

# Dynamic Helicity Control of Oligo(salamo)-Based Metal Helicates

Shigehisa Akine <sup>1,2</sup> 

<sup>1</sup> Graduate School of Natural Science and Technology, Kanazawa University, Kanazawa 920-1192, Japan; akine@se.kanazawa-u.ac.jp; Tel.: +81-76-264-5701

<sup>2</sup> Nano Life Science Institute, Kanazawa University, Kanazawa 920-1192, Japan

Received: 5 July 2018; Accepted: 10 August 2018; Published: 17 August 2018



**Abstract:** Much attention has recently focused on helical structures that can change their helicity in response to external stimuli. The requirements for the invertible helical structures are a dynamic feature and well-defined structures. In this context, helical metal complexes with a labile coordination sphere have a great advantage. There are several types of dynamic helicity controls, including the responsive helicity inversion. In this review article, dynamic helical structures based on oligo(salamo) metal complexes are described as one of the possible designs. The introduction of chiral carboxylate ions into  $Zn_3La$  tetranuclear structures as an additive is effective to control the *P/M* ratio of the helix. The dynamic helicity inversion can be achieved by chemical modification, such as protonation/deprotonation or desilylation with fluoride ion. When (*S*)-2-hydroxypropyl groups are introduced into the oligo(salamo) ligand, the helicity of the resultant complexes is sensitively influenced by the metal ions. The replacement of the metal ions based on the affinity trend resulted in a sequential multistep helicity inversion. Chiral salen derivatives are also effective to bias the helicity; by incorporating the *gauche/anti* transformation of a 1,2-disubstituted ethylene unit, a fully predictable helicity inversion system was achieved, in which the helicity can be controlled by the molecular lengths of the diammonium guests.

**Keywords:** helical structure; dynamic structure conversion; responsive molecule; metal complex; salen ligand; helicity control; helicity inversion; chirality switch

## 1. Introduction

### 1.1. Dynamic Helical Structures

In supramolecular chemistry, non-covalent interactions are effectively utilized for obtaining thermodynamically-favored self-assembled structures thanks to reversible processes [1,2]. Among the various types of non-covalent interactions, metal coordination has a great advantage to make the desired structures because of their well-defined geometry and high directionality of the coordination structures. The representative examples are self-assembled coordination compounds, such as macrocycles, cages, giant spheres, etc. [3–5].

Non-covalent interactions also play an important role in the formation of higher-order structures, which are found in biomolecules such as proteins and nucleic acids. One of the ubiquitously found higher-order structures in biomolecules is the helical structure, such as  $\alpha$ -helix of proteins and complementary double helix in nucleic acids. These helical structures could have a dynamic feature because they are spontaneously formed from flexible molecules via reversible processes and maintained by non-covalent interactions. While the advantage of static helical structures, such as helicenes [6–10], is to provide a stable chiral field that would remain intact irrespective of the environment, it would sometimes be advantageous to construct dynamic helical structures that

can change their chirality depending on the situations (Figure 1). In this context, dynamic helical structures that are spontaneously constructed by non-covalent interactions would be useful to achieve responsive functions.

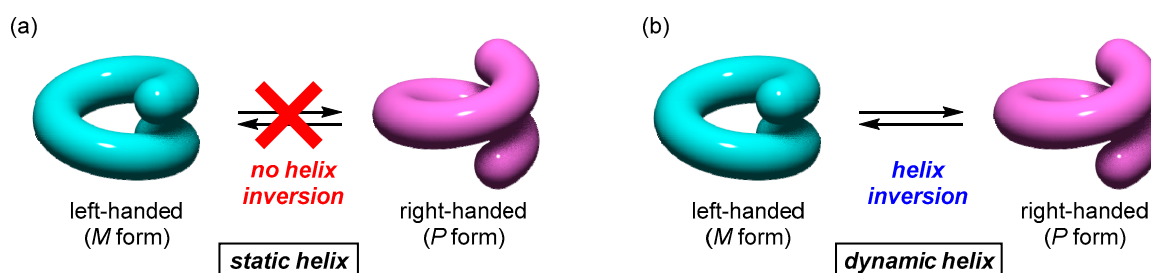


**Figure 1.** The *P* and *M* forms of (a) static and (b) dynamic helical structures.

There are several types of dynamic helical structures based on artificial molecular scaffolds. For example, foldamers [11] are acyclic molecules that can spontaneously form a higher-order structure under certain conditions by non-covalent interactions, such as hydrogen bonding, solvophobic effects, electrostatic interactions, etc., while they adopt a random coil conformation under undesired conditions. On the other hand, more stable helical structures can be obtained by metal coordination, which are useful for obtaining well-defined structures. The chemistry of helical structures based on metal coordination has been initiated from the self-assembled double helicates that are obtained by complexation of oligobipyridine ligands with metal ions [12]. To date, various kinds of helical structures including single-, double-, and triple-helicates have been synthesized by metal complexation from the appropriate organic structures containing multiple coordination sites and linkers [13,14].

### 1.2. Helicity Control of Dynamic Helical Structures

Helical structures have a helicity of right-handed (*P* helix) and left-handed (*M* helix), which are the mirror image of each other. Those obtained by helical folding of achiral molecules are racemic in solution, because there is no kinetic or thermodynamic preference to the *P* or *M* form. In this situation, we do not expect chemical and physical functions derived from the helical chirality, because chiral functions based on the *P* and *M* forms are cancelled by each other. Nevertheless, the inherently chiral feature of helical molecules is attractive to enable new chiral functions, and it should be important to obtain helical structures as the one-handed form.

In general, each of the enantiomers of an organic molecule having a chiral carbon atom can be separated by optical resolution of the racemic mixture. Organic chemists have developed various methods for optical resolution via diastereomeric salt formation, chiral HPLC, spontaneous resolution, etc. [15]. However, these methods cannot be used to separate an enantiomer pair of dynamic helical molecules, because they undergo interconversion among the *P* and *M* forms, sometimes via random coil structures, etc. (Figure 2). This means that there is a racemization pathway, which produces an equimolar mixture of the *P* and *M* enantiomers.

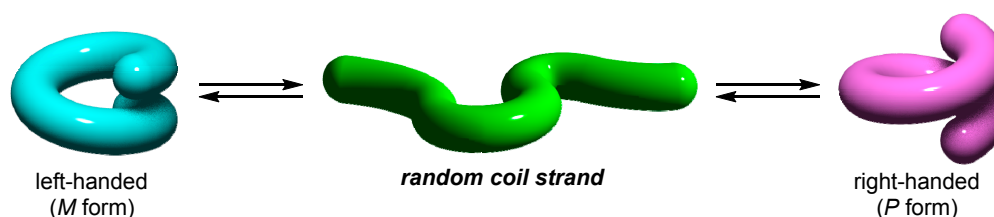


**Figure 2.** Interconversion between *P* and *M* forms of a helical structure via a random coil structure.

If we need a one-handed helix of a dynamic helical structure in solution, we have to shift the  $P/M$  equilibrium from 50:50 (racemic). Since the energies of an enantiomer pair are exactly the same (Figure 3a), we have to convert the enantiomer pair into a diastereomer pair by the introduction of a chiral auxiliary. In this case, the  $P/M$  equilibrium ratio deviates from 50:50 due to the difference in the thermodynamic stabilities (Figure 3b). If the chiral group is relatively small compared with the helix, we can shift the equilibrium while keeping the  $P$  and  $M$  helices as the approximate mirror image of each other. This is the basic concept of the dynamic helicity control, which has been used to obtain one-handed forms of various dynamic helical structures such as metal helicates and helical polymers [16,17]. Since the  $P$  and  $M$  forms are in dynamic equilibrium, we can change the  $P/M$  equilibrium ratio by the addition/removal or modification of the chiral auxiliary. This would lead to responsive helicity changes and inversions as described in Section 1.3, which are recognized as one of the hot topics in functional molecular chemistry [18–24].

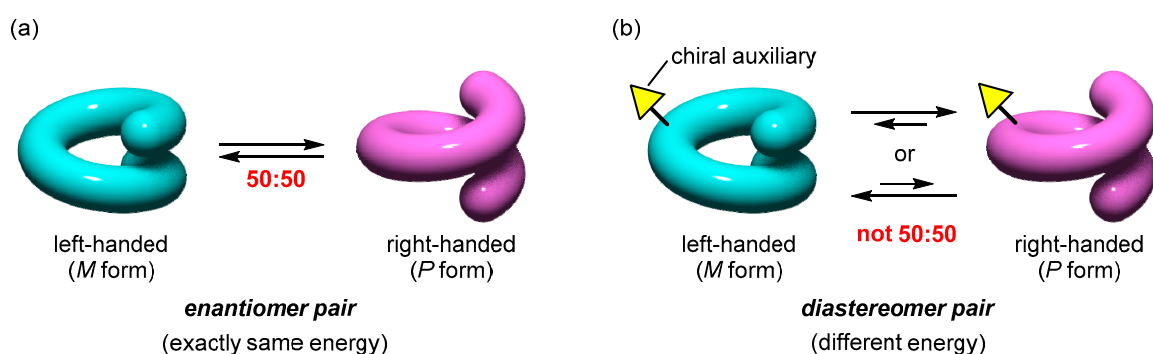


**Figure 3.** Equilibrium between  $P$  and  $M$  forms and their energy differences. (a) Enantiomer pair, (b) diastereomer pair.

### 1.3. Classification of Helicity Control and Helicity Inversion of Dynamic Helical Metal Complexes

In this article, we describe the helicity control and helicity inversion of dynamic single-helical structures that are obtained by the complexation of acyclic organic ligands with the appropriate metal ions. In the helicity control phenomena, the changes in the helicity can be discussed in terms of the changes in the  $P/M$  ratios, which correspond to the stability difference in the right- and the left-handed forms. Depending on whether the chirality is introduced in the helical structures or the chemical stimuli, the helicity changes are classified into the following three categories A, B, and C.

- Category A. Formation of helical structures with a biased  $P/M$  ratio.

In this case, helical structures with a biased  $P/M$  ratio are obtained upon the helix formation by the metal complexation of an acyclic ligand having a chiral auxiliary (Figure 4a). The chiral auxiliary that is pre-installed into the helix scaffold causes the deviation of the  $P/M$  ratio from 50:50 as a result of the thermodynamic equilibration, because the introduction of the chiral auxiliary converts the  $P/M$  enantiomer pair into a diastereomer pair.

- Category B. Shift of the 50:50  $P/M$  ratios of racemic helical structures.

In this case, stimuli-responsiveness is introduced so that the exactly 50:50  $P/M$  ratio of a racemic helical structure is biased upon the addition of a chiral auxiliary as an additive (Figure 4b). A chiral stimulus converts the enantiomer pair into a diastereomer pair, which causes the dynamic shift of the  $P/M$  equilibrium. This change is regarded as the helicity induction triggered by a chiral additive, which can be detected by the induced CD signal.

- Category C. Increase, decrease, or inversion of  $P/M$  ratios by chemical modification.

In this case, stimuli-responsiveness is used for helicity changes such as helicity inversion. For example, the  $P/M$  ratio is changed by replacing or modifying the chiral auxiliary (Figure 4c). If the pre-installed chiral auxiliary becomes more effective after the modification, the helical biases should be increased. If the chiral auxiliary after the modification stabilizes the opposite helicity from the original form, a responsive helicity inversion is expected. The helicity change can also be achieved without altering the chiral auxiliary, by using chemical stimuli such as achiral ions (Figure 4d). If the structures of a helix framework are chemically modified, the  $P/M$  preference is also changed even if the chiral auxiliary is unchanged. Therefore, for a helix having a pre-installed chiral auxiliary, the  $P/M$  equilibrium ratio can be increased, decreased, or inverted upon stimulation with the suitable achiral additive.

Among the dynamic helicity changing phenomena reported so far, responsive helicity inversion is attracting much attention because this would be used to switch various kinds of chiral functions. These are principally based on Category C in Figure 4. To date, various types of chemical and other stimuli have been used to achieve dynamic helicity inversion of the helical structures such as polymers, metal helicates, etc. [18–24].

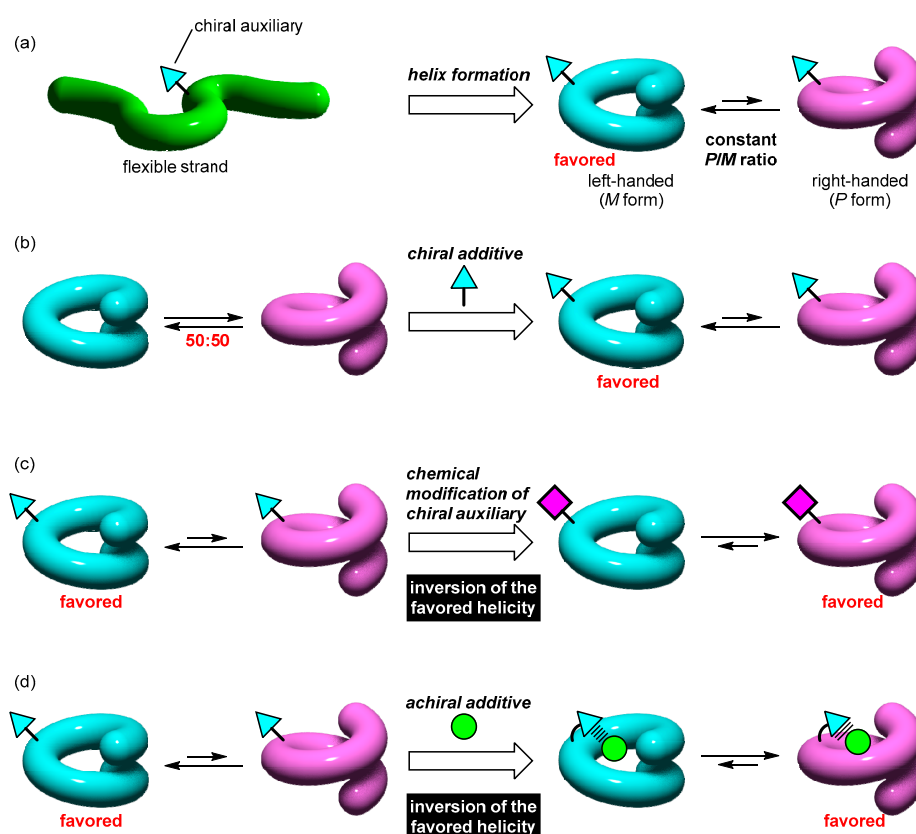


**Figure 4.** Typical strategies for dynamic helicity control. (a) Formation of a dynamic helical structure from a flexible ligand having a chiral auxiliary (Category A). (b) Equilibrium shift from a racemic helix (Category B). (c) Helicity inversion using chemical modification of the chiral auxiliary (Category C). (d) Helicity inversion using an achiral additive (Category C). The turquoise triangles represent a chiral auxiliary that stabilizes the left-handed forms.

## 2. Molecular Design of Oligo(salen)-Type Helical Structures

### 2.1. Molecular Design

As one of the possible candidates of dynamic helical complexes, we designed metal complexes having a series of acyclic oligo(salen)-type ligands ( $H_2\text{salen} = N,N'$ -disalicylideneethylenediamine)

(Figure 5a) [25–30], while there are several types of related helical structures based on monomeric [31–41], dimeric [42,43] and polymeric [44–46] salen-type ligands. We employed salamo derivatives, the oxime analog of salen, as the constituent of the oligomers ( $H_2\text{salamo} = 1,2\text{-bis(salicylideneaminoxyl)ethane}$ ) [47,48]. The salamo ligands show a high stability to suppress the  $C=N$  bond recombination to facilitate the synthesis of acyclic salamo oligomers, keeping the tetradentate coordination ability for various transition metals [49–55]. When each of the salamo units in an oligo(salamo) ligand accommodates a metal ion in a tetradentate fashion, its structure is fixed in a curved conformation due to the newly formed coordination bonds (Figure 5b). If all of the salamo units are metalated, a single-helical structure would be spontaneously formed (Figure 5c). The reversibility of the coordination bonds in labile metal complex moieties would afford a dynamic feature, which allows interconversion between the *P* and *M* forms (and sometimes random coil structures as well) (Figure 2).

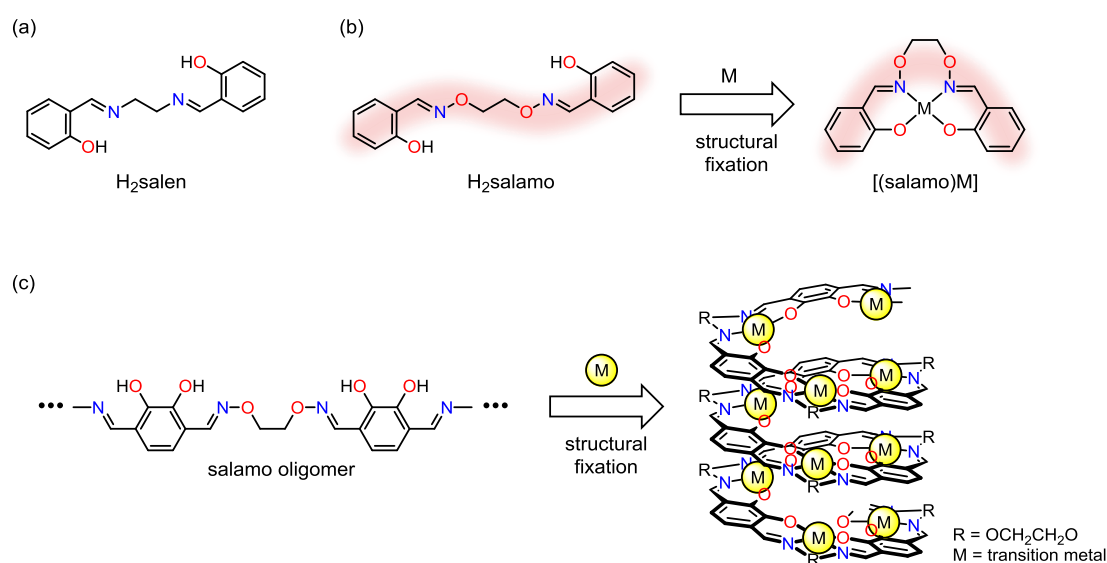


**Figure 5.** (a) Structure of  $H_2\text{salen}$ . (b) Conformational change of  $H_2\text{salamo}$  upon metalation. (c) Molecular design of an oligo(salamo) ligand for construction of single-helical structures upon metalation.

## 2.2. Construction of Helical Structures and Their Dynamic Helix Inversion Behavior

The shortest oligomer, the acyclic bis(salamo) ligand  $H_4L^1$ , forms the trinuclear helical complex  $L^1Zn_2M$  upon the complexation with zinc(II) acetate in the presence of a guest ion  $M^{n+}$  (=alkaline earth metals, rare earth metals) (Figure 6) [56,57]. The helix winding angle, which is defined as the sum of five  $O-M-O$  angles, is changed between 289 deg ( $M^{n+} = La^{3+}$ ) and 345 deg ( $M^{n+} = Sc^{3+}$ ), depending on the ionic radius of the guest ion  $M^{n+}$  [57]. These angles correspond to less than one-turn helix, which does not lead to an efficient overlap of the two terminal benzene rings. Therefore, these helical complexes are generally fluxional and the helix inversion is fast.

If the oligomer chains are elongated, the helix winds more and the terminals are more efficiently overlapped, so that the helix inversion would be less favorable [58,59]. Indeed, the complexation of the tris(salamo) ligand  $H_6L^2$  with  $Zn^{2+}$  and  $M^{n+}$  ( $=La^{3+}$ ,  $Ba^{2+}$ ) afforded larger single-helical complexes,  $L^2Zn_3M$  [58,60] (Figure 6). The crystallographic analysis revealed that the helix winding angle of  $[L^2Zn_3La(OAc)_3]$  is 421 deg, which nearly corresponds to 1.2 turns. Due to the efficient overlap of the two terminals, the helix inversion does not seem to take place without partial dissociation of the coordination bonds. Indeed, the helix inversion rates of these helical tetranuclear complexes depended on the central metal ions [60].  $L^2Zn_3Ba$  undergoes a fast helix inversion on the  $^1H$  NMR timescale while  $L^2Zn_3La$  undergoes a slow helix inversion, but  $L^2Zn_3La$  still has a dynamic feature due to the

reversible coordination bonds (see below). This indicates that the helicity inversion processes involve cleavage of some of the coordination bonds.

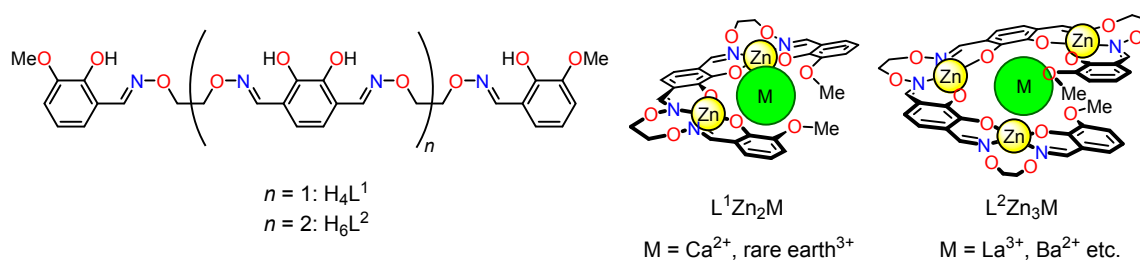


**Figure 6.** Oligo(salamo) ligands ( $H_4L^1$  and  $H_6L^2$ ) and molecular structures of the helical complexes ( $L^1Zn_2M$  and  $L^2Zn_3M$ ).

### 3. Dynamic Helicity Control by Chiral Counteranions

#### 3.1. Strategy

In this section, we describe the control of the helicity, e.g.,  $P/M$  ratios, of the oligo(salamo)-based helical structures, by the introduction of a chiral auxiliary via coordination bonds. When the  $P$  and  $M$  enantiomers of a dynamic helix are in equilibrium in solution, introduction of a chiral auxiliary would shift the equilibrium, as described as Category B (Figure 4) in Section 1.3. Preferential formation of one of the  $P$  and  $M$  helices is expected as a result of the dynamic equilibration.

Since acetate ions readily coordinate to the multimetallic core of the oligo(salamo) helical complexes [57,58,60], chiral carboxylate ions should be one of the promising candidates as a chiral auxiliary (Figure 7). An equilibrium shift is expected if there is a significant difference in the thermodynamic stabilities of the  $P$  and  $M$  diastereomers. In order to avoid the competition among the counteranions, triflate salts,  $[L^1Zn_2La](OTf)_3$  and  $[L^2Zn_3La](OTf)_3$ , were used as the starting complexes instead of the acetate salts. We investigated the changes in the  $P/M$  ratios upon the addition of chiral carboxylate ions such as hydroxy acids and amino acids.

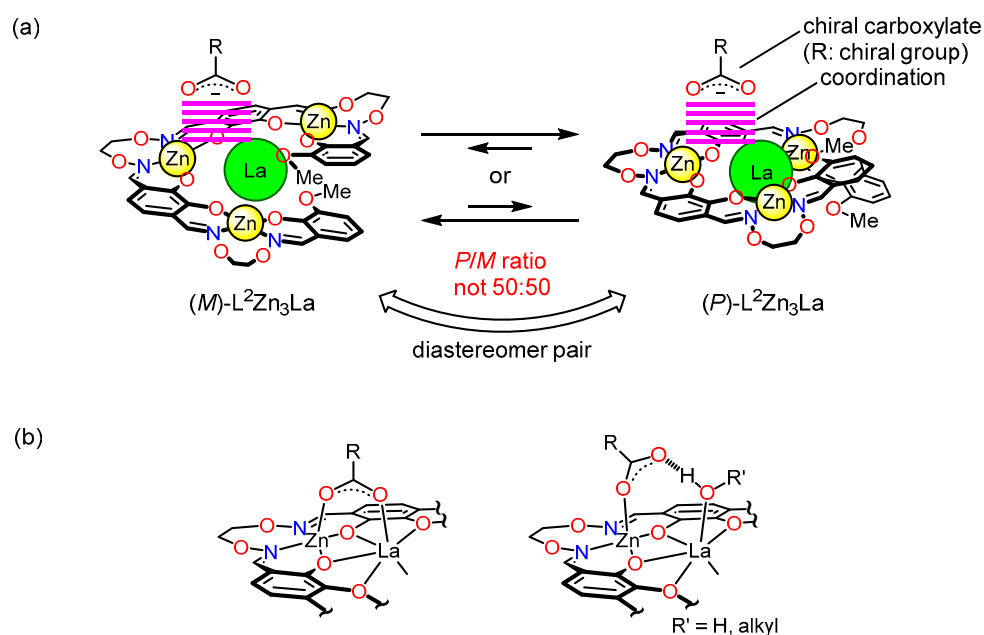


**Figure 7.** (a) Helicity control of  $L^2Zn_3La$  by coordination of chiral carboxylate ions (Category B in Figure 4). (b) Two major coordination modes of carboxylate ions to the Zn–La core found in crystal structures of related complexes.

### 3.2. Helicity Control Using Hydroxy Acids

The efficiency of the dynamic helicity control of  $L^1Zn_2La$  and  $L^2Zn_3La$  by the coordination with chiral hydroxy acids (Category B in Figure 4) was investigated by CD spectroscopy. When mandelic acid and DABCO as a base were present, both complexes showed CD signals, which are indicative of the biased  $P/M$  ratios. In particular, the tetranuclear analogue,  $L^2Zn_3La$ , showed a more intense CD signal at 350 nm, which is ascribed to the  $\pi-\pi^*$  absorption. The negative CD at 350 nm corresponds to the  $M$  helix (see Section 5.2). The sign and intensity of the CD signal are sensitively influenced by the structure  $R$  in the hydroxy acids  $R-CH(OH)-CO_2^-$ . A negative CD signal was observed for  $R = Ph$ ,  $PhCH_2CH_2$ ,  $Me$  at around 350 nm, while a positive CD signal was observed for  $R = PhCH_2$  (Figure 8). The CD intensity was almost proportional to the diastereomeric excesses ranging from 42% to 56%, which were determined by  $^1H$  NMR spectroscopy ( $P/M = 71:29$  to  $22:78$ ) [61].

The titration study and the Job plot analysis indicated that two carboxylate ions can coordinate to one  $L^2Zn_3La$  tetranuclear core, while only one carboxylic acid molecule can coordinate to a bis(saloph) helix, reported by Kleij, to induce a CD signal [42]. Interestingly, the helicity-controlling efficiency of the mandelate ion in the second step was 3.6 times higher than that in the first step. This leads to the non-linear response in the CD intensity changes, e.g., helicity changes, upon the binding with a carboxylate ion [61]. This is related to the chirality amplification found in some dynamic polymers and supramolecular assemblies, which is one of the recent hot topics in chemistry of responsive molecules [62–64].

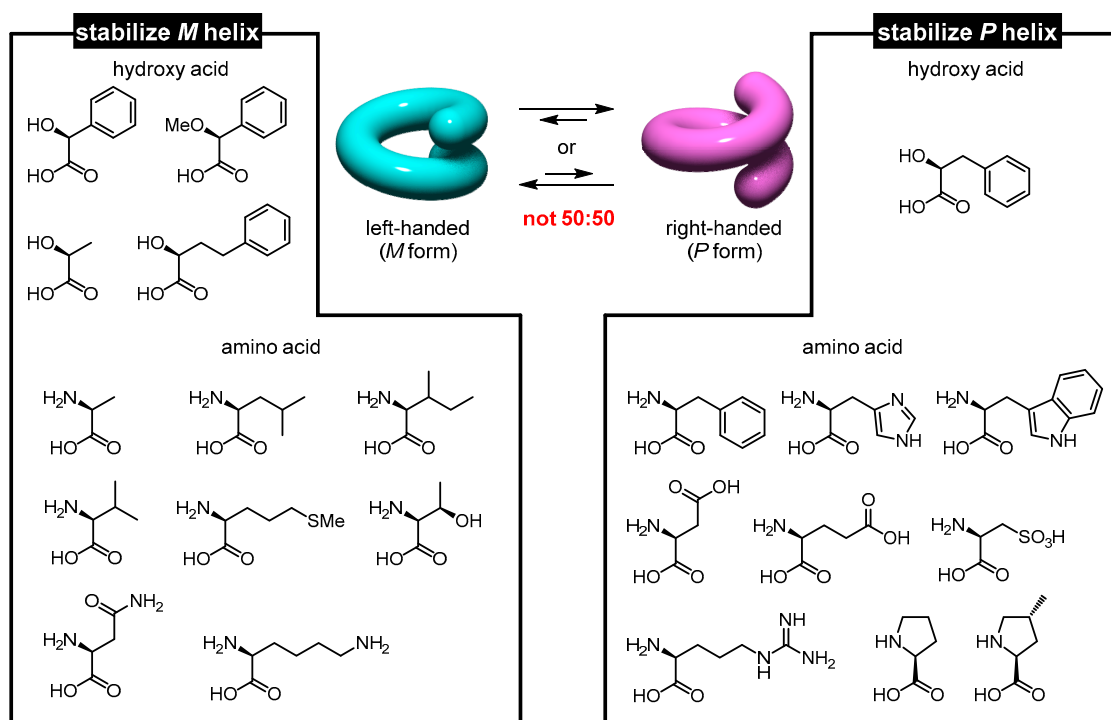


**Figure 8.** Helicity control of  $L^2Zn_3La$  by the coordination of hydroxy acid/DABCO (3 equivalent each) or amino acid (3 equivalent).

### 3.3. Helicity Control Using Amino Acids

$\alpha$ -Amino acid derivatives are known as an easily accessible series of chiral compounds that can induce the helical bias of helical structures such as polymers and helicates [65–69]. They can also be used to shift the  $P/M$  equilibrium of the helical tetranuclear complex,  $L^2Zn_3La$ , in a similar manner. As observed for hydroxy acids, the CD sign and intensity are sensitively influenced by the structure  $R$

in the amino acids,  $R\text{-CH}(\text{NH}_3^+)\text{-CO}_2^-$  [70] (Figure 8). Aliphatic amino acids (Ala, Leu, Ile, Val, Met) induced a negative CD signal at 350 nm, while aromatic ones (Phe, His, Trp) induced a positive CD.

It is well known that some amino acids have residues that can change their structure upon protonation/deprotonation by acid and base. Such a structural conversion would change the helicity-controlling ability, so that an increase, decrease, or inversion of the  $P/M$  ratio is expected (Category C in Figure 4). Indeed, the CD signal decreased upon deprotonation of the coordinating Glu by the addition of DABCO (+22.0 to +8.6 mdeg) and increased upon deprotonation of the coordinating Pro and Hyp. In the case of cysteic acid, the positive CD was inverted to negative upon the addition of DABCO (+16.9 to  $-9.3$  mdeg) [70]. This means that the helicity was inverted upon the deprotonation. A repeated helicity inversion is also achieved by the alternate addition of TfOH and DABCO (Figure 9). While some responsive polymer systems having acidic or basic groups undergo helicity inversion upon pH changes [71–73], there are rare examples of a pH-responsive helicity inversion of discrete helical molecules. This is the first helicity inversion system based on a discrete molecule in which the helicity inversion is driven by structural changes in the non-covalently attached chiral auxiliary.

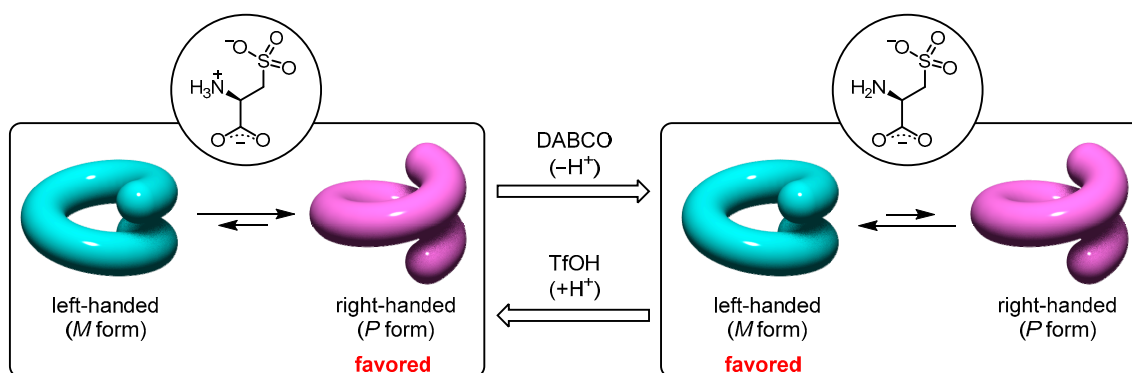


**Figure 9.** Responsive helicity inversion observed in the  $L^2Zn_3La$ /cysteic acid system driven by protonation/deprotonation.

### 3.4. Dynamic Helicity Inversion by Chemical Modifications

Since the  $P/M$  ratios are sensitively influenced by the structures of the coordinating carboxylate ions, a responsive helicity control can be achieved by chemical modification of the carboxylate ions (Category B in Figure 4). As seen in the protonation/deprotonation by the TfOH/DABCO combination, the carboxylate ions before and after the chemical modification should stabilize the opposite helicities of  $L^2Zn_3La$ . We found that TBDMS-protected  $\alpha$ -hydroxy carboxylate ions efficiently work for this purpose. The TBDMS groups can be removed by fluoride ion. In addition, the hydroxy carboxylate ions (**H1**, **H2**) and the corresponding TBDMS-protected analogues (**S1**, **S2**) are found to induce opposite helicities in acetonitrile/chloroform (9:1). Therefore, the removal of the TBDMS group in the siloxycarboxylate (**S1**, **S2**) by fluoride ion would cause the helicity inversion.

Indeed, responsive helicity inversion was observed upon the addition of fluoride ion to the  $L^2Zn_3La$  solution containing silyloxy lactate ions **S1** [74] (Figure 10). The negative CD signal at 350 nm gradually weakened and inverted to the positive signal, which clearly indicates that the TBDMS removal caused the helicity inversion. Interestingly, when mandelate derivative **S2** was used as the siloxycarboxylate ion, the CD intensity change became significantly slower.

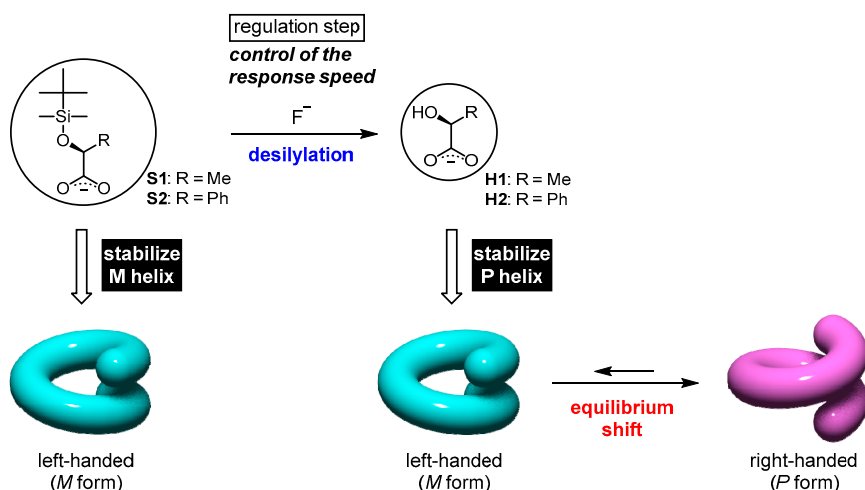


**Figure 10.** Response speed control of helicity inversion of  $L^2Zn_3La$  using desilylation of coordinating siloxycarboxylate ions (S1, S2).

Usually, response speeds of most artificial responsive molecules are constant under a certain condition, because the response speeds are principally determined by the rate of the structural conversion such as a chemical reaction and isomerization. In this case, however, the response speeds can be strategically and efficiently tuned by the reactivity of the siloxycarboxylate ions at the regulation step, just like regulatory enzymes in biological systems [75]. This type of response speed control would be useful for developing new functional molecules and materials that would change their functions in a time-programmable fashion.

#### 4. Dynamic Helicity Control by Chiral Tethers

##### 4.1. Strategy

While we can easily introduce a chiral auxiliary into helical structures by coordination bonds, the resulting helicity and its efficiency are sometimes difficult to predict mainly because there is a binding equilibrium between the chiral auxiliary and the helical structure. In addition, it is sometimes difficult to know how the chiral auxiliary is interacting with the helical scaffold. We expected that the interactions are more predictable if we can directly introduce the chiral auxiliary via covalent bonds instead of non-covalent interactions. Here, 2-hydroxypropyl groups are directly introduced as the chiral auxiliary into the acyclic oligo(salamo) ligand framework (Figure 11) [76,77]. When suitable metal ions are introduced into the  $H_4L^3$  and  $H_6L^4$  ligands having this chiral group, the resultant helical complexes should have a  $P/M$  ratio that deviates from 50:50 (Category A in Figure 4). This chiral group would efficiently interact with the metal centers in the helical complexes via direct coordination or the hydrogen bonding to the coordinating counter anions.

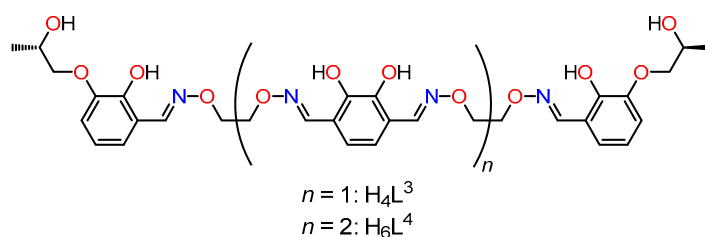


**Figure 11.** Molecular design of bis- and tris(salamo) ligands,  $H_4L^3$  and  $H_6L^4$ , having chiral tethers, (*S*)-2-hydroxypropyl groups.

#### 4.2. Helicity Control of Helical Complexes

The bis- and tris(salamo) ligands ( $H_4L^3$  and  $H_6L^4$ ) having (*S*)-2-hydroxypropyl groups were synthesized and converted to the helical complexes,  $L^3Zn_2M$  and  $L^4Zn_3M$ , respectively. The trinuclear complex,  $L^3Zn_2M$ , obtained from the shorter analogue,  $H_4L^3$ , undergoes a fast helix inversion on the  $^1H$  NMR timescale at room temperature. The NMR study at 223 K indicates that the *P/M* ratio of  $L^3Zn_2Ca$  was the most efficiently biased (80:20), while those for the rare earth metal complexes are not efficiently biased (56:44 for  $L^3Zn_2Y$ ; 53:47 for  $L^3Zn_2La$ ) [76].

In contrast, the longer analogue  $H_6L^4$  formed tetranuclear complexes  $L^4Zn_3M$  that can undergo a slow helix inversion on the  $^1H$  NMR timescale at room temperature. In the CD spectrum of  $L^4Zn_3La$ , an intense negative signal was observed at around 350 nm, which is indicative of the *M* helix. The  $L^4Zn_3La$  complex showed the diastereomeric ratio of *P/M* = 26:74, which was determined by  $^1H$  NMR spectroscopy, and  $L^4Zn_3Ba$  showed only one set of  $^1H$  NMR signals. This indicated that the (*S*)-2-hydroxypropyl group is an efficient chiral auxiliary for the helicity control of  $L^4Zn_3M$ . Interestingly, the CD spectrum of the  $L^4Zn_3Ba$  complex showed a positive signal at around 350 nm, which was opposite to that of  $L^4Zn_3La$ . Therefore, the (*S*)-2-hydroxypropyl group affects the helical framework of  $L^4Zn_3M$  to produce different helicities depending on the central metal ions  $M^{n+}$  [77] (Figure 12).

The helicity was more precisely and finely tuned by taking advantage of the lanthanide contraction, e.g., systematic size variation of a series of 15 lanthanide(III) ions [78]. The CD signal of  $L^4Zn_3M$  was monotonically increased from  $La^{3+}$  to  $Sm^{3+}$  to give the maximum *P/M* ratio for  $M = Sm^{3+}$  (*P/M* = 17:83). The CD intensity decreased from  $Sm^{3+}$  to  $Lu^{3+}$ , which was explained by the formation of a partially coiled structure as a side product.

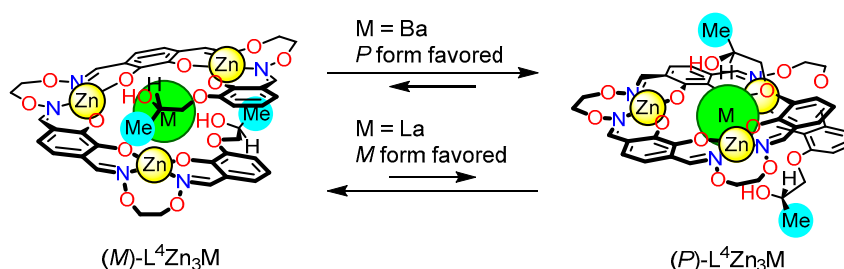


**Figure 12.** Dynamic equilibrium between *P* and *M* forms of tetranuclear complex  $L^4Zn_3M$  that has tris(salamo) ligand  $L^4$  with (*S*)-2-hydroxypropyl groups as the chiral auxiliary (Category A in Figure 4).

#### 4.3. Helicity Inversion by Metal Exchange

Since the helicities of  $L^4Zn_3La$  and  $L^4Zn_3Ba$  are different from each other, it is interesting to know the helicity changes when the metal ion  $M^{n+}$  in  $L^4Zn_3M$  is replaced by another (Category C in Figure 4). We have already demonstrated that a binding selectivity trend of alkali metal  $\ll Zn^{2+} <$  alkaline earth  $<$  rare earth metal ions was observed in the shorter  $L^1Zn_2M$  system [57] and related complexes [79–83] without chiral auxiliary. If the longer  $L^4Zn_3M$  system having a chiral auxiliary also shows a similar selectivity trend,  $Ba^{2+}$  in the  $L^4Zn_3Ba$  can be efficiently replaced by  $La^{3+}$ . It is also expected that a multistep conversion can be achieved when more than two kinds of metal ions are sequentially added according to the affinity order.

Indeed, a multistep conversion from the  $Zn^{2+}$  complex to the  $Ba^{2+}$  complex then the  $La^{3+}$  complex was achieved [77] (Figure 13). The complexation of the free ligand,  $H_6L^4$ , with  $Zn^{2+}$  afforded two kinds of complexes,  $L^4Zn_3$  and  $L^4Zn_5$ , which unexpectedly showed opposite CD signals. When up to 3 equivalent. of  $Zn^{2+}$  were present, a positive CD signal was observed at 332 nm due to the formation of  $L^4Zn_3$ . However, the further addition of 2 equivalent. of  $Zn^{2+}$  resulted in inversion of the CD signal, giving a negative CD signal at 348 nm due to the formation of  $L^4Zn_5$ . This clearly indicated

that the helicity was inverted from *P* to *M*. In this pentanuclear complex,  $L^4Zn_5$ , three  $Zn^{2+}$  ions are located at the salamo chelate moieties while the other two are accommodated in the central  $O_8$  site. These two central  $Zn^{2+}$  ions can be replaced by  $Ba^{2+}$  to yield the heterometallic  $L^4Zn_3Ba$  complex, which shows a positive CD signal at 354 nm indicative of the *P* helicity. As expected from the affinity order, the  $Ba^{2+}$  ion was completely replaced by  $La^{3+}$  to yield the  $L^4Zn_3La$  complex, which shows a negative CD signal at 352 nm. Therefore, the helicity inversion took place three times in a sequential fashion based on a multistep metal exchange protocol. Such a sequential and multistep conversion feature of the helicity inversion would be useful as a multifunction control system that can switch different kinds of asymmetric functions upon each helicity inversion.

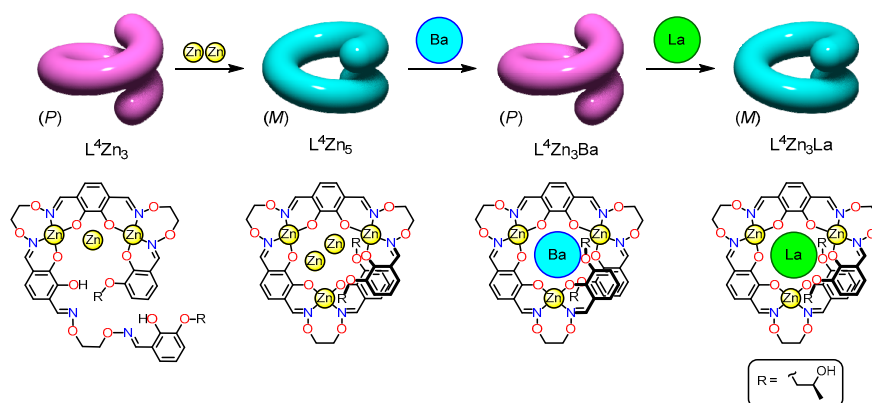


**Figure 13.** Three-step conversion among metal complexes,  $L^4Zn_3$ ,  $L^4Zn_5$ ,  $L^4Zn_3Ba$ , and  $L^4Zn_3La$ , associated with sequential helicity inversion.

## 5. Dynamic Helicity Control Using Chiral Salen Units

### 5.1. Strategy

In the previous two sections, helicity control by using chiral carboxylate ions or covalently-linked chiral tethers was described. In both methods, the *P/M* ratios of the metal complexes were sensitively influenced by the changes in the environment and thus difficult to predict from the molecular structures of the organic framework. In order to control the helicity in a more rational and predictable fashion, we focused on chiral salen derivatives, which have two chiral carbon centers at the ethylene bridge of the salen ligands. It is well known that some chiral salen complexes act as excellent enantioselective catalysts (up to 99% ee) [84–87] and this indicates that the *chiral twist* is perfectly controlled in these systems. The *chiral twist* can be discussed in terms of the N–C–C–N dihedral angles (+60 deg or –60 deg) of the ethylene bridge in the salen ligands. The +60 deg dihedral angle of the ethylene units makes the *chiral twist* of the metallosalen unit that is better fit to the *M* helix, while the –60 deg to the *P* helix (Figure 14).

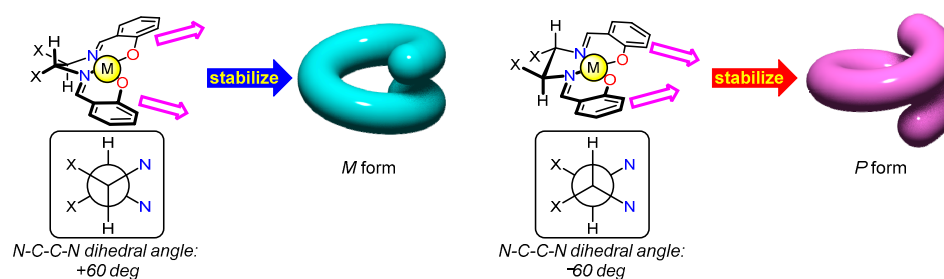


**Figure 14.** The *chiral twist* of the chiral salen complexes that can control the helicity. The salen complexes having +60 and –60 deg dihedral angle better fit and more stabilize the *M*- and *P*-helices, respectively.

### 5.2. Dynamic Helicity Control of Chiral Salen Units

As the chiral constituents, we used two kinds of chiral ethylene bridges, *trans*-1,2-diphenylethane-1,2-diyl ( $L^5$ ) and *trans*-1,2-cyclohexanediyyl ( $L^6$ ) groups, which were easily derived from the corresponding commercially-available diamines. From the molecular modeling studies, the *M* form of the oligo(salamo)  $Zn_3M$  helix seems to be less distorted when the *R,R*-configuration is used (Figure 15). Therefore, we expected that ligands  $H_6L^5$  and  $H_6L^6$  would afford the *M* helix as the major conformer when suitable metal ions are introduced (Category A in Figure 4).

The equilibrated *P/M* ratios of  $L^5Zn_3La$  and  $L^6Zn_3La$  were 29:71 and 13:87, respectively, which were determined by  $^1H$  NMR analysis [88,89]. As expected, the *M* form was the major isomer for both complexes judging from the negative CD signal at around 350 nm (see below). Thus, we can control the helicity as predicted from the molecular structure based on the N–C–C–N dihedral angles, and demonstrated that the chiral salen structure was effective for predictable helicity control.

While there are both the *P* and *M* forms in solution of  $L^5Zn_3La$  (*P/M* = 29:71 in equilibrium), the crystallization of this complex from chloroform afforded crystals containing only the *M* form (Figure 16a) [88]. When the crystals of this isolated (*M*)- $L^5Zn_3La$  were dissolved in chloroform/methanol (1:1), the pure *M* form gradually changed into a *P/M* mixture in the initial ratio of 29:71. The half-life of the *P/M* isomerization was determined to be 43.7 min by CD spectroscopy.

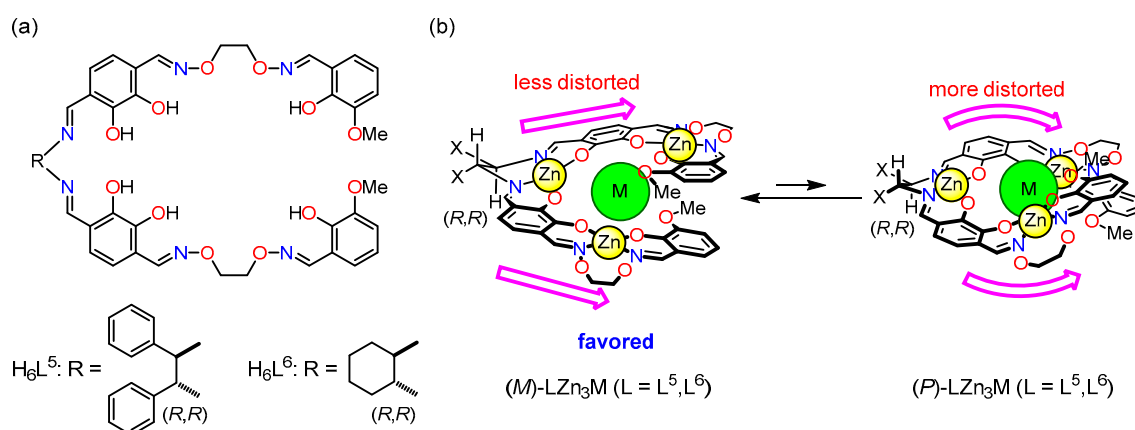


**Figure 15.** (a) Molecular structures of chiral ligands,  $H_6L^5$  and  $H_6L^6$ . (b) Concept of the predictable helicity control by using chiral salen unit (Category A in Figure 4).

The X-ray crystallographic analysis indicated that the molecular structure of  $L^5Zn_3La$  was very similar to that of the related complex  $L^2Zn_3La$  having no chiral auxiliary. Interestingly, the *M* helical tetranuclear complex  $L^5Zn_3La$  formed a helical array in the crystal lattice and the helical array is left-handed due to the  $P4_3$  space group in the tetragonal crystal system [88]. This can be regarded as a helix-of-helix structure in which left-handed helical subunits formed a left-handed helical array. Therefore, the chiral auxiliary of the  $L^5Zn_3La$  controls the helical chirality not only in the helical subunit but also in the helical array (Figure 16a). This type of hierarchical chirality control has been reported in very limited systems [90], but this would be important for structural control in various types of hierarchical systems.

In contrast to  $L^5Zn_3La$ , the 1,2-cyclohexanediyyl analogue  $L^6Zn_3La$  formed quasiracemic crystals, which contain *P* and *M* forms in an exact 1:1 ratio, although the *M* form is significantly favored in an equilibrated solution (*P/M* = 13:87) (Figure 16b) [89]. The space group was  $C2$  in the monoclinic system, which is lacking the inversion centers or glide planes, but the packing structure of this crystal is quite similar to that of the centrosymmetric  $C2/c$  space group. Similar quasiracemic crystals were also obtained in the case of  $L^6NiZn_2La$  [91]. The *P/M* ratio of  $L^6NiZn_2La$  was almost perfectly biased to the *M* form in the chloroform/methanol (1:1) solution.

In the crystal structure of  $L^6Zn_3La$ , the  $P$  and  $M$  diastereomers are approximately related by an apparent inversion center, and the molecular structures of the  $P$  and  $M$  forms are also the approximate mirror image of each other except for the *trans*-1,2-cyclohexanediyl moiety as a chiral auxiliary. In addition, the chiroptical properties are almost the mirror image of each other, because the solution immediately after the dissolution of the crystals was almost CD silent. The CD intensity gradually increased to the level of the equilibrated mixture containing the  $P$  and  $M$  forms in a 13:87 ratio [89]. A noteworthy feature in this system is that the chiral auxiliary is effective in shifting the  $P/M$  ratio in solution although the  $P$  and  $M$  forms behave like an enantiomer pair in the crystallization process and in their photophysical properties. In this sense, this crystal is nearly a “racemic” crystal, in which only the  $P/M$  equilibrium ratio deviates from 50:50. Consequently, when we dissolve the quasiracemic crystals of  $L^6Zn_3La$ , the 50:50  $P/M$  ratio spontaneously shifts to the initial ratio ( $P/M = 13:87$ ). This phenomenon seems to be a spontaneous enrichment of the  $M$  form if we focus only on the helical chirality that is observable by CD spectroscopy (Figure 16b).

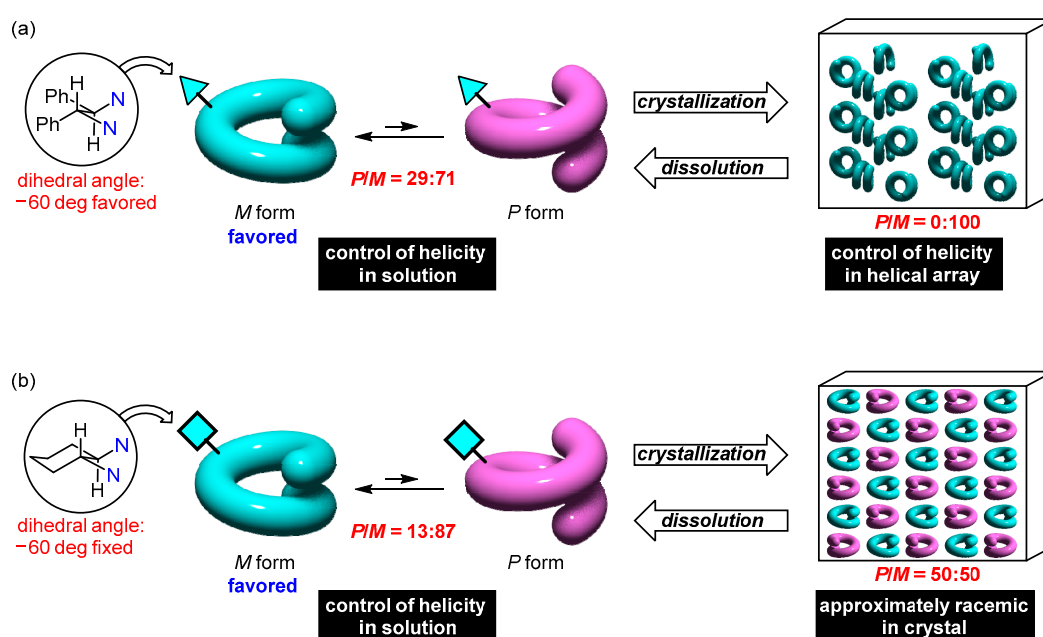


**Figure 16.** The  $P/M$  ratios of (a)  $L^5Zn_3La$  and (b)  $L^6Zn_3La$  in solution and in the crystal.

### 5.3. Helicity Inversion by Leverage Mechanism

As already mentioned, the introduction of chiral salen units was effective to control the helicity of the single helix in a predictable fashion based on the organic molecular structures. In this molecular design, the *chiral twist*, the N–C–C–N dihedral angle of  $+60$  or  $-60$  deg in the *trans*-1,2-disubstituted ethylene group, determines the preferred helicity of  $P$  or  $M$ . Consequently, we can change the preferred helicity in conjunction with the change in the dihedral angle between  $+60$  and  $-60$  deg. In the case of the (*S,S*)-stereoconfiguration, the  $P$  form is favored when the dihedral angle is set to  $+60$  deg, which corresponds to the *gauche* position of the two substituents. On the other hand, the  $M$  form is favored when the dihedral angle is set to  $-60$  deg, which corresponds to the *anti* position. Since the distances between the two substituents in the *gauche* and *anti* positions are significantly different from each other, it is expected that we can change the helicity by extending and shortening the distance. Thus we designed a new ligand  $H_6L^7$ , having two benzo-18-crown-6 units in the *trans*-1,2-disubstituted ethylene bridge [92]. The interaction of  $L^7Zn_3La$  with diammonium guests changes the distance between the two crown units so that short and long diammonium guests would stabilize the  $P$  and  $M$  forms, respectively (Category C in Figure 4) (Figure 17).

When 1,4-butanediammonium salt is added as a short diammonium guest, the two crown units are fixed in the *gauche* position, which should stabilize the *P* helix. As expected, the enrichment of the *P* helix was clearly evidenced by the increase in the positive CD intensity at 352 nm and the increase of the *P*/*M* ratio from 75:25 to 85:15 was confirmed by  $^1\text{H}$  NMR spectroscopy, although the *P* helix is already favored even in the absence of the diammonium guest due to the *trans*-1,2-bis(crown)-substituted ethylene bridge.

On the other hand, when longer 1,12-dodecanediammonium guest is added, the *anti* conformation of the two crown units should be stabilized to give the *M* form as the favored structure. The helicity inversion from the *P* to *M* helix was evident by the disappearance of the positive CD signal and concomitant emergence of the negative CD signal at 362 nm. The helicity inversion was also clearly demonstrated by the change in the *P*/*M* ratio from 75:25 to 34:66, which was determined by  $^1\text{H}$  NMR spectroscopy.

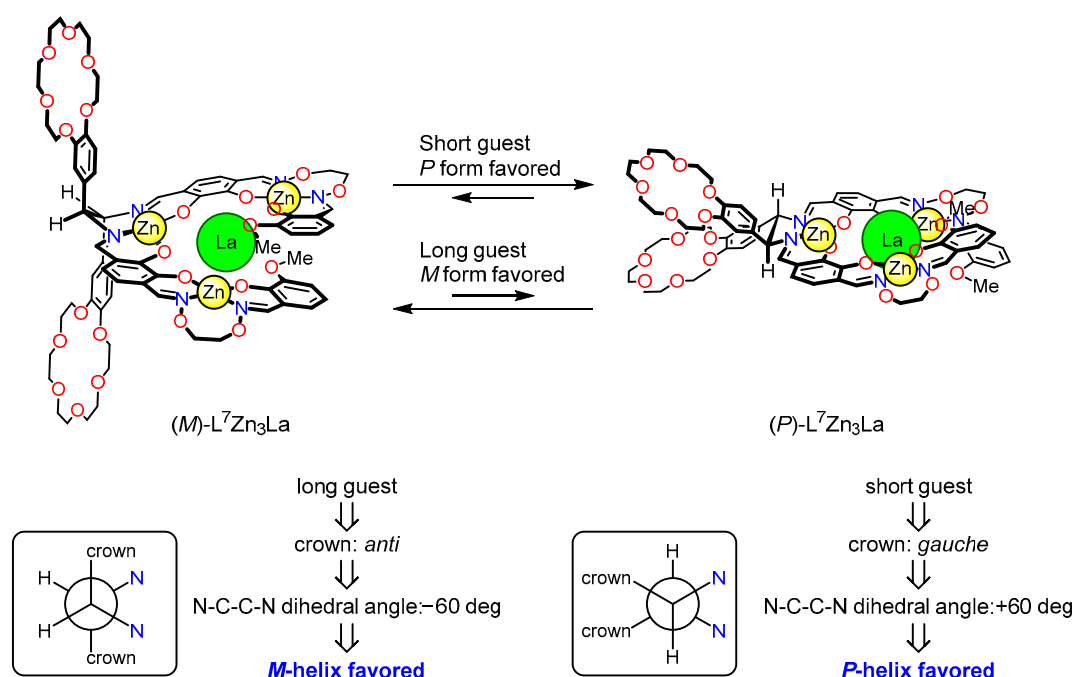


**Figure 17.** Molecular design of helical complex  $\text{L}^7\text{Zn}_3\text{La}$  having two crown units for predictable helicity control and inversion based on chiral salen structure.

Therefore, the  $\text{L}^7\text{Zn}_3\text{La}$  tetranuclear system having two crown units acted as a new helicity control/inversion system, in which the two crown units can remotely control the helicity like a leverage mechanism [92]. The favored helicity was determined by the molecular lengths of the diammonium salts. The 1,2-disubstituted ethylene bridge was an effective converter that can change the information of molecular lengths into the chirality information.

## 6. Conclusions

A series of single-helical structures were obtained by the complexation of bis- and tris(salamo) ligands with metal ions. The helical structures showed a dynamic feature that allows interconversion between the *P* and *M* forms, which can be explained by the labile characters of the coordination structures. The introduction of a chiral auxiliary, such as chiral carboxylate ions, chiral tethers, and a chiral salen unit, was effective to shift the *P*/*M* equilibrium from 50:50. In particular, the 1,2-disubstituted ethylene bridge in the chiral salen unit facilitated the synthesis of dynamic helical structures in which the preferred helicity is rationally predicted from the structure of the organic framework. In addition to the oligo(salamo) helical structures reported in this article,

there have already been a number of reports on various kinds of helical structures based on the monomeric [31–41], dimeric [42,43] and polymeric [44–46] salen-type ligands, as well as the tris(saloph) triple-helical cages [93,94] and single-helix with different types of donor sets [90,95–97]. It has already been demonstrated that the oligo(salamo) helical complexes show unique physical properties and reactivities [98–101], and the dynamic helicity control would be useful for switching of the chiroptical properties of the helical structures. The catalytic reactivity of the chiral metallosalen scaffold [84–87] could also be incorporated into the oligo(salamo) helical structures, which could dynamically switch the enantioselectivity of the catalytic reactions. In this sense, the oligo(salen)-type helical structures are promising to provide an excellent platform that can drive the dynamic switching of various kinds of chiral functions.

**Funding:** This research was funded by JSPS KAKENHI (Nos. 18H03913, 16H06510, 26288022, and 23750055), Grant for Basic Science Research Projects from Sumitomo Foundation, Kanazawa University CHOZEN project, and the World Premier International Research Center Initiative (WPI), MEXT, Japan.

**Acknowledgments:** The author thanks Tatsuya Nabeshima (University of Tsukuba) for valuable discussion to do researches on the project of oligo(salamo) helical structures. In particular, he expresses his gratitude for Takanori Taniguchi, Takashi Matsumoto, Sayaka Hotate, and Shiho Sairenji, who have worked on the studies of helicity control.

**Conflicts of Interest:** The author declares no conflict of interest.

## References

1. Lehn, J.-M. *Supramolecular Chemistry Concepts and Perspectives*; VCH: Weinheim, Germany, 1995; ISBN 3-527-29311-6.
2. Steed, J.W.; Atwood, J.L. *Supramolecular Chemistry*; Wiley: Chichester, UK, 2000; ISBN 0-471-98791-3.
3. Fujita, M.; Tominaga, M.; Hori, A.; Therrien, B. Coordination Assemblies from a Pd(II)-Cornered Square Complex. *Acc. Chem. Res.* **2005**, *38*, 371–380. [[CrossRef](#)] [[PubMed](#)]
4. Chakrabarty, R.; Mukherjee, P.S.; Stang, P.J. Supramolecular Coordination: Self-Assembly of Finite Two- and Three-Dimensional Ensembles. *Chem. Rev.* **2011**, *111*, 6810–6918. [[CrossRef](#)] [[PubMed](#)]
5. McConnell, A.J.; Wood, C.S.; Neelakandan, P.P.; Nitschke, J.R. Stimuli-Responsive Metal–Ligand Assemblies. *Chem. Rev.* **2015**, *115*, 7729–7793. [[CrossRef](#)] [[PubMed](#)]
6. Shen, Y.; Chen, C.-F. Helicenes: Synthesis and Applications. *Chem. Rev.* **2012**, *112*, 1463–1535. [[CrossRef](#)] [[PubMed](#)]
7. Gingras, M. One hundred years of helicene chemistry. Part 1: Non-stereoselective syntheses of carbohelicenes. *Chem. Soc. Rev.* **2013**, *42*, 968–1006. [[CrossRef](#)] [[PubMed](#)]
8. Gingras, M.; Félix, G.; Peresutti, R. One hundred years of helicene chemistry. Part 2: Stereoselective syntheses and chiral separations of carbohelicenes. *Chem. Soc. Rev.* **2013**, *42*, 1007–1050. [[CrossRef](#)] [[PubMed](#)]
9. Gingras, M. One hundred years of helicene chemistry. Part 3: Applications and properties of carbohelicenes. *Chem. Soc. Rev.* **2013**, *42*, 1051–1095. [[CrossRef](#)] [[PubMed](#)]
10. Starý, I.; Stará, I.G.; Alexandrová, Z.; Sehnal, P.; Teplý, F.; Šaman, D.; Rulišek, L. Helicity control in the synthesis of helicenes and related compounds. *Pure Appl. Chem.* **2006**, *78*, 495–499. [[CrossRef](#)]
11. Hill, D.J.; Mio, M.J.; Prince, R.B.; Hughes, T.S.; Moore, J.S. A Field Guide to Foldamers. *Chem. Rev.* **2001**, *101*, 3893–4011. [[CrossRef](#)] [[PubMed](#)]
12. Lehn, J.-M.; Rigault, A.; Siegel, J.; Harrowfield, J.; Chevrier, B.; Moras, D. Spontaneous assembly of double-stranded helicates from oligobipyridine ligands and copper(I) cations: Structure of an inorganic double helix. *Proc. Natl. Acad. Sci. USA* **1987**, *84*, 2565–2569. [[CrossRef](#)] [[PubMed](#)]
13. Pigué, C.; Bernardinelli, G.; Hopfgartner, G. Helicates as Versatile Supramolecular Complexes. *Chem. Rev.* **1997**, *97*, 2005–2062. [[CrossRef](#)] [[PubMed](#)]
14. Albrecht, M. “Let’s Twist Again”—Double-Stranded, Triple-Stranded, and Circular Helicates. *Chem. Rev.* **2001**, *101*, 3457–3497. [[CrossRef](#)] [[PubMed](#)]
15. Porter, W.H. Resolution of chiral drugs. *Pure Appl. Chem.* **1991**, *63*, 1119–1122. [[CrossRef](#)]
16. Yashima, E.; Maeda, K.; Iida, H.; Furusho, Y.; Nagai, K. Helical Polymers: Synthesis, Structures, and Functions. *Chem. Rev.* **2009**, *109*, 6102–6211. [[CrossRef](#)] [[PubMed](#)]

17. Yashima, E.; Ousaka, N.; Taura, D.; Shimomura, K.; Ikai, T.; Maeda, K. Supramolecular Helical Systems: Helical Assemblies of Small Molecules, Foldamers, and Polymers with Chiral Amplification and Their Functions. *Chem. Rev.* **2016**, *116*, 13752–13990. [[CrossRef](#)] [[PubMed](#)]
18. Miyake, H.; Tsukube, H. Helix Architecture and Helicity Switching via Dynamic Metal Coordination Chemistry. *Supramol. Chem.* **2005**, *17*, 53–59. [[CrossRef](#)]
19. Miyake, H.; Tsukube, H. Coordination chemistry strategies for dynamic helicates: Time-programmable chirality switching with labile and inert metal helicates. *Chem. Soc. Rev.* **2012**, *41*, 6977–6991. [[CrossRef](#)] [[PubMed](#)]
20. Crassous, J. Transfer of chirality from ligands to metal centers: Recent examples. *Chem. Commun.* **2012**, *48*, 9684–9692. [[CrossRef](#)] [[PubMed](#)]
21. Maeda, K.; Yashima, E. Helical Polyacetylenes Induced via Noncovalent Chiral Interactions and Their Applications as Chiral Materials. *Top. Curr. Chem.* **2017**, *375*, 72. [[CrossRef](#)] [[PubMed](#)]
22. Bisoyi, H.K.; Li, Q. Light-Directed Dynamic Chirality Inversion in Functional Self-Organized Helical Superstructures. *Angew. Chem. Int. Ed.* **2016**, *55*, 2994–3010. [[CrossRef](#)] [[PubMed](#)]
23. Pijper, D.; Feringa, B.L. Control of dynamic helicity at the macro- and supramolecular level. *Soft Matter* **2008**, *4*, 1349–1372. [[CrossRef](#)]
24. Feringa, B.L.; van Delden, R.A.; Koumura, N.; Geertsema, E.M. Chiroptical Molecular Switches. *Chem. Rev.* **2000**, *100*, 1789–1816. [[CrossRef](#)] [[PubMed](#)]
25. Akine, S.; Nabeshima, T. Cyclic and acyclic oligo(N<sub>2</sub>O<sub>2</sub>) ligands for cooperative multi-metal complexation. *Dalton Trans.* **2009**, 10395–10408. [[CrossRef](#)] [[PubMed](#)]
26. Akine, S. Novel Ion Recognition Systems Based on Cyclic and Acyclic Oligo(salen)-type Ligands. *J. Incl. Phenom. Macrocycl. Chem.* **2012**, *72*, 25–54. [[CrossRef](#)]
27. Akine, S. Metal Complexes with Oligo(salen)-Type Ligands. In *The Chemistry of Metal Phenolates, Volume 2, Patai's Chemistry of Functional Groups*; Zabicky, J., Ed.; John Wiley and Sons, Ltd.: Chichester, UK, 2018; pp. 153–194, ISBN 978-1-119-08328-3.
28. Wezenberg, S.J.; Kleij, A.W. Material Applications for Salen Frameworks. *Angew. Chem. Int. Ed.* **2008**, *47*, 2354–2364. [[CrossRef](#)] [[PubMed](#)]
29. Kleij, A.W. New Templating Strategies with Salen Scaffolds (Salen = *N,N'*-Bis(salicylidene)ethylenediamine Dianion). *Chem. Eur. J.* **2008**, *14*, 10520–10529. [[CrossRef](#)] [[PubMed](#)]
30. Feltham, H.L.C.; Brooker, S. Ligands and polymetallic complexes derived from 1,4-diformyl-2,3-dihydroxybenzene and two close analogues. *Coord. Chem. Rev.* **2009**, *253*, 1458–1475. [[CrossRef](#)]
31. Wiznycia, A.V.; Desper, J.; Levy, C.J. Iron(II) and zinc(II) monohelical binaphthyl salen complexes. *Chem. Commun.* **2005**, 4693–4695. [[CrossRef](#)] [[PubMed](#)]
32. Wiznycia, A.V.; Desper, J.; Levy, C.J. Monohelical Iron(II) and Zinc(II) Complexes of a (1*R*,2*R*)-Cyclohexyl Salen Ligand with Benz[*a*]anthryl Sidearms. *Inorg. Chem.* **2006**, *45*, 10034–10036. [[CrossRef](#)] [[PubMed](#)]
33. Wiznycia, A.V.; Desper, J.; Levy, C.J. Iron(II) and zinc(II) monohelical binaphthyl-salen complexes with overlapping benz[*a*]anthryl sidearms. *Dalton Trans.* **2007**, 1520–1527. [[CrossRef](#)] [[PubMed](#)]
34. Barman, S.; Patil, S.; Desper, J.; Aikens, C.M.; Levy, C.J. Helical Oxidovanadium(IV) Salen-Type Complexes: Synthesis, Characterisation and Catalytic Behaviour. *Eur. J. Inorg. Chem.* **2013**, 5708–5717. [[CrossRef](#)]
35. Zhang, F.; Bai, S.; Yap, G.P.A.; Tarwade, V.; Fox, J.M. Abiotic Metallofoldamers as Electrochemically Responsive Molecules. *J. Am. Chem. Soc.* **2005**, *127*, 10590–10599. [[CrossRef](#)] [[PubMed](#)]
36. Dong, Z.; Karpowicz, R.J., Jr.; Bai, S.; Yap, G.P.A.; Fox, J.M. Control of Absolute Helicity in Single-Stranded Abiotic Metallofoldamers. *J. Am. Chem. Soc.* **2006**, *128*, 14242–14243. [[CrossRef](#)] [[PubMed](#)]
37. Dong, Z.; Yap, G.P.A.; Fox, J.M. *trans*-Cyclohexane-1,2-diamine is a Weak Director of Absolute Helicity in Chiral Nickel–Salen Complexes. *J. Am. Chem. Soc.* **2007**, *129*, 11850–11853. [[CrossRef](#)] [[PubMed](#)]
38. Fisher, L.A.; Zhang, F.; Yap, G.P.A.; Fox, J.M. Weak absolute helicity direction in Ni–salen by *trans*-cyclohexane-(1*R*,2*R*)-diamine. *Inorg. Chim. Acta* **2010**, *364*, 259–260. [[CrossRef](#)]
39. Dong, Z.; Plampin, J.N., III; Yap, G.P.A.; Fox, J.M. Minimalist End Groups for Control of Absolute Helicity in Salen- and Salophen-Based Metallofoldamers. *Org. Lett.* **2010**, *12*, 4002–4005. [[CrossRef](#)] [[PubMed](#)]
40. Dong, Z.; Bai, S.; Yap, G.P.A.; Fox, J.M. Interplay between the diamine structure and absolute helicity in Ni–salen metallofoldamers. *Chem. Commun.* **2011**, *47*, 3781–3783. [[CrossRef](#)] [[PubMed](#)]
41. Mizukami, S.; Houjou, H.; Nagawa, Y.; Kanetsato, M. First helical zinc(II) complex with a salen ligand. *Chem. Commun.* **2003**, 1148–1149. [[CrossRef](#)]

42. Wezenberg, S.J.; Salassa, G.; Escudero-Adán, E.C.; Benet-Buchholz, J.; Kleij, A.W. Effective Chirogenesis in a Bis(metallosalphen) Complex through Host–Guest Binding with Carboxylic Acids. *Angew. Chem. Int. Ed.* **2011**, *50*, 713–716. [[CrossRef](#)] [[PubMed](#)]
43. Achira, H.; Ito, M.; Mutai, T.; Yoshikawa, I.; Araki, K.; Houjou, H. Spontaneous helical folding of bis(Ni-salphen) complexes in solution and in the solid state: Spectroscopic tracking of the unfolding process induced by Na<sup>+</sup> ions. *Dalton Trans.* **2014**, *43*, 5899–5907. [[CrossRef](#)] [[PubMed](#)]
44. Dai, Y.; Katz, T.J.; Nichols, D.A. Synthesis of a Helical Conjugated Ladder Polymer. *Angew. Chem. Int. Ed. Engl.* **1996**, *35*, 2109–2111. [[CrossRef](#)]
45. Zhang, H.-C.; Huang, W.-S.; Pu, L. Biaryl-Based Macrocyclic and Polymeric Chiral (Salophen)Ni(II) Complexes: Synthesis and Spectroscopic Study. *J. Org. Chem.* **2001**, *66*, 481–487. [[CrossRef](#)] [[PubMed](#)]
46. Furusho, Y.; Maeda, T.; Takeuchi, T.; Makino, N.; Takata, T. A Rational Design of Helix: Absolute Helix Synthesis by Binaphthyl-Salen Fusion. *Chem. Lett.* **2001**, 1020–1021. [[CrossRef](#)]
47. Akine, S.; Taniguchi, T.; Nabeshima, T. Synthesis and Characterization of Novel Ligands 1,2-Bis(salicylideneaminoxy)ethanes. *Chem. Lett.* **2001**, 682–683. [[CrossRef](#)]
48. Akine, S.; Taniguchi, T.; Dong, W.; Masubuchi, S.; Nabeshima, T. Oxime-Based Salen-Type Tetradentate Ligands with High Stability against Imine Metathesis Reaction. *J. Org. Chem.* **2005**, *70*, 1704–1711. [[CrossRef](#)] [[PubMed](#)]
49. Akine, S.; Taniguchi, T.; Nabeshima, T. Cooperative Formation of Trinuclear Zinc(II) Complexes via Complexation of a Tetradentate Oxime Chelate Ligand, Salamo, and Zinc(II) Acetate. *Inorg. Chem.* **2004**, *43*, 6142–6144. [[CrossRef](#)] [[PubMed](#)]
50. Akine, S.; Nabeshima, T. Novel Thiosalamo Ligand as a Remarkably Stable N<sub>2</sub>S<sub>2</sub> Salen-type Chelate and Synthesis of a Nickel(II) Complex. *Inorg. Chem.* **2005**, *44*, 1205–1207. [[CrossRef](#)] [[PubMed](#)]
51. Akine, S.; Taniguchi, T.; Nabeshima, T. Heterometallic Zn<sub>2</sub>La and ZnLu Complexes Formed by Site-selective Transmetalation of a Dimeric Homotrinnuclear Zinc(II) Complex. *Chem. Lett.* **2006**, *35*, 604–605. [[CrossRef](#)]
52. Akine, S.; Dong, W.; Nabeshima, T. Octanuclear Zinc(II) and Cobalt(II) Clusters Produced by Cooperative Tetrameric Assembling of Oxime Chelate Ligands. *Inorg. Chem.* **2006**, *45*, 4677–4684. [[CrossRef](#)] [[PubMed](#)]
53. Akine, S.; Akimoto, A.; Shiga, T.; Oshio, H.; Nabeshima, T. Synthesis, Stability, and Complexation Behavior of Isolable Salen-Type N<sub>2</sub>S<sub>2</sub> and N<sub>2</sub>SO Ligands Based on Thiol and Oxime Functionalities. *Inorg. Chem.* **2008**, *47*, 875–885. [[CrossRef](#)] [[PubMed](#)]
54. Akine, S.; Utsuno, F.; Taniguchi, T.; Nabeshima, T. Dinuclear Complexes of the N<sub>2</sub>O<sub>2</sub> Oxime Chelate Ligand with Zinc(II)–Lanthanide(III) as a Selective Sensitization System for Sm<sup>3+</sup>. *Eur. J. Inorg. Chem.* **2010**, 3143–3152. [[CrossRef](#)]
55. Akine, S.; Nabeshima, T. Increased Nuclearity of Salen-Type Transition Metal Complexes by Incorporation of O-Alkyloxime Functionality. *Heteroat. Chem.* **2014**, *25*, 410–421. [[CrossRef](#)]
56. Akine, S.; Taniguchi, T.; Nabeshima, T. Novel Synthetic Approach to Trinuclear 3d–4f Complexes: Specific Exchange of the Central Metal of a Trinuclear Zinc(II) Complex of a Tetraoxime Ligand with a Lanthanide(III) Ion. *Angew. Chem. Int. Ed.* **2002**, *41*, 4670–4673. [[CrossRef](#)] [[PubMed](#)]
57. Akine, S.; Taniguchi, T.; Nabeshima, T. Helical Metallohost–Guest Complexes via Site-Selective Transmetalation of Homotrinnuclear Complexes. *J. Am. Chem. Soc.* **2006**, *128*, 15765–15774. [[CrossRef](#)] [[PubMed](#)]
58. Akine, S.; Taniguchi, T.; Saiki, T.; Nabeshima, T. Ca<sup>2+</sup>- and Ba<sup>2+</sup>-Selective Receptors Based on Site-Selective Transmetalation of Multinuclear Polyoxime–Zinc(II) Complexes. *J. Am. Chem. Soc.* **2005**, *127*, 540–541. [[CrossRef](#)] [[PubMed](#)]
59. Akine, S.; Matsumoto, T.; Sairenji, S.; Nabeshima, T. Synthesis of Acyclic Tetrakis- and Pentakis(N<sub>2</sub>O<sub>2</sub>) Ligands for Single-helical Heterometallic Complexes with a Greater Number of Winding Turns. *Supramol. Chem.* **2011**, *23*, 106–112. [[CrossRef](#)]
60. Akine, S.; Taniguchi, T.; Matsumoto, T.; Nabeshima, T. Guest-dependent inversion rate of a tetranuclear single metallohelicate. *Chem. Commun.* **2006**, 4961–4963. [[CrossRef](#)] [[PubMed](#)]
61. Sairenji, S.; Akine, S.; Nabeshima, T. Dynamic helicity control of single-helical oligooxime metal complexes by coordination of chiral carboxylate ions. *Tetrahedron Lett.* **2014**, *55*, 1987–1990. [[CrossRef](#)]
62. Green, M.M.; Peterson, N.C.; Sato, T.; Teramoto, A.; Cook, R.; Lifson, S. A Helical Polymer with a Cooperative Response to Chiral Information. *Science* **1995**, *268*, 1860–1866. [[CrossRef](#)] [[PubMed](#)]

63. Palmans, A.R.A.; Meijer, E.W. Amplification of Chirality in Dynamic Supramolecular Aggregates. *Angew. Chem. Int. Ed.* **2007**, *46*, 8948–8968. [[CrossRef](#)] [[PubMed](#)]
64. Nagata, Y.; Yamada, T.; Adachi, T.; Akai, Y.; Yamamoto, T.; Suginome, M. Solvent-Dependent Switch of Helical Main-Chain Chirality in Sergeants-and-Soldiers-Type Poly(quinoxaline-2,3-diyl)s: Effect of the Position and Structures of the “Sergeant” Chiral Units on the Screw-Sense Induction. *J. Am. Chem. Soc.* **2013**, *135*, 10104–10113. [[CrossRef](#)] [[PubMed](#)]
65. Mizutani, T.; Yagi, S.; Honmaru, A.; Murakami, S.; Furusyo, M.; Takagishi, T.; Ogoshi, H. Helical Chirality Induction in Zinc Bilindiones by Amino Acid Esters and Amines. *J. Org. Chem.* **1998**, *63*, 8769–8784. [[CrossRef](#)]
66. Mizutani, T.; Sakai, N.; Yagi, S.; Takagishi, T.; Kitagawa, S.; Ogoshi, H. Allosteric Chirality Amplification in Zinc Bilinone Dimer. *J. Am. Chem. Soc.* **2000**, *122*, 748–749. [[CrossRef](#)]
67. Nonokawa, R.; Yashima, E. Detection and Amplification of a Small Enantiomeric Imbalance in  $\alpha$ -Amino Acids by a Helical Poly(phenylacetylene) with Crown Ether Pendants. *J. Am. Chem. Soc.* **2003**, *125*, 1278–1283. [[CrossRef](#)] [[PubMed](#)]
68. Sakai, R.; Otsuka, I.; Satoh, T.; Kakuchi, R.; Kaga, H.; Kakuchi, T. Thermoresponsive On–Off Switching of Chiroptical Property Induced in Poly(4'-ethynylbenzo-15-crown-5)/ $\alpha$ -Amino Acid System. *Macromolecules* **2006**, *39*, 4032–4037. [[CrossRef](#)]
69. Misaki, H.; Miyake, H.; Shinoda, S.; Tsukube, H. Asymmetric Twisting and Chirality Probing Properties of Quadruple-Stranded Helicates: Coordination Versatility and Chirality Response of  $\text{Na}^+$ ,  $\text{Ca}^{2+}$ , and  $\text{La}^{3+}$  Complexes with Octadentate Cyclen Ligand. *Inorg. Chem.* **2009**, *48*, 11921–11928. [[CrossRef](#)] [[PubMed](#)]
70. Sairenji, S.; Akine, S.; Nabeshima, T. Dynamic Helicity Control of a Single-Helical Oligooxime Complex and Acid–Base-triggered Repeated Helicity Inversion Mediated by Amino Acids. *Chem. Lett.* **2014**, *43*, 1107–1109. [[CrossRef](#)]
71. Sanji, T.; Kato, N.; Tanaka, M. Switching of Optical Activity in Oligosilane through pH-Responsive Chiral Wrapping with Amylose. *Macromolecules* **2006**, *39*, 7508–7512. [[CrossRef](#)]
72. Maeda, T.; Furusho, Y.; Sakurai, S.-I.; Kumaki, J.; Okoshi, K.; Yashima, E. Double-Stranded Helical Polymers Consisting of Complementary Homopolymers. *J. Am. Chem. Soc.* **2008**, *130*, 7938–7945. [[CrossRef](#)] [[PubMed](#)]
73. Janssen, P.G.A.; Ruiz-Carretero, A.; González-Rodríguez, D.; Meijer, E.W.; Schenning, A.P.H.J. pH-Switchable Helicity of DNA-Templated Assemblies. *Angew. Chem. Int. Ed.* **2009**, *48*, 8103–8106. [[CrossRef](#)] [[PubMed](#)]
74. Sairenji, S.; Akine, S.; Nabeshima, T. Response speed control of helicity inversion based on a “regulatory enzyme”-like strategy. *Sci. Rep.* **2018**, *8*, 137. [[CrossRef](#)] [[PubMed](#)]
75. Traut, T.W. *Allosteric Regulatory Enzymes*; Springer: New York, NY, USA, 2008; ISBN 0-387-72888-0.
76. Akine, S.; Taniguchi, T.; Nabeshima, T. Chiral single-stranded metallohelix: Metal-mediated folding of linear oligooxime ligand. *Tetrahedron Lett.* **2006**, *47*, 8419–8422. [[CrossRef](#)]
77. Akine, S.; Sairenji, S.; Taniguchi, T.; Nabeshima, T. Stepwise Helicity Inversions by Multisequential Metal Exchange. *J. Am. Chem. Soc.* **2013**, *135*, 12948–12951. [[CrossRef](#)] [[PubMed](#)]
78. Sairenji, S.; Akine, S.; Nabeshima, T. Lanthanide contraction for helicity fine-tuning and helix-winding control of single-helical metal complexes. *Dalton Trans.* **2016**, *45*, 14902–14906. [[CrossRef](#)] [[PubMed](#)]
79. Akine, S.; Kagiya, S.; Nabeshima, T. Modulation of Multimetal Complexation Behavior of Tetraoxime Ligand by Covalent Transformation of Olefinic Functionalities. *Inorg. Chem.* **2010**, *49*, 2141–2152. [[CrossRef](#)] [[PubMed](#)]
80. Akine, S.; Morita, Y.; Utsuno, F.; Nabeshima, T. Multiple Folding Structures Mediated by Metal Coordination of Acyclic Multidentate Ligand. *Inorg. Chem.* **2009**, *48*, 10670–10678. [[CrossRef](#)] [[PubMed](#)]
81. Akine, S.; Tadokoro, T.; Nabeshima, T. Oligometallic Template Strategy for Synthesis of a Macrocyclic Dimer-Type Octaoxime Ligand for Its Cooperative Complexation. *Inorg. Chem.* **2012**, *51*, 11478–11486. [[CrossRef](#)] [[PubMed](#)]
82. Akine, S.; Sunaga, S.; Nabeshima, T. Multistep Oligometal Complexation of the Macrocyclic Tris( $\text{N}_2\text{O}_2$ ) Hexaoxime Ligand. *Chem. Eur. J.* **2011**, *17*, 6853–6861. [[CrossRef](#)] [[PubMed](#)]
83. Akine, S.; Sunaga, S.; Taniguchi, T.; Miyazaki, H.; Nabeshima, T. Core/Shell Oligometallic Template Synthesis of Macrocyclic Hexaoxime. *Inorg. Chem.* **2007**, *46*, 2959–2961. [[CrossRef](#)] [[PubMed](#)]
84. Canali, L.; Sherrington, D.C. Utilisation of homogeneous and supported chiral metal(salen) complexes in asymmetric catalysis. *Chem. Soc. Rev.* **1999**, *28*, 85–93. [[CrossRef](#)]

85. Ito, Y.N.; Katsuki, T. Asymmetric Catalysis of New Generation Chiral Metallosalen Complexes. *Bull. Chem. Soc. Jpn.* **1999**, *72*, 603–619. [[CrossRef](#)]
86. Jacobsen, E.N. Asymmetric Catalysis of Epoxide Ring-Opening Reactions. *Acc. Chem. Res.* **2000**, *33*, 421–431. [[CrossRef](#)] [[PubMed](#)]
87. Baleizão, C.; Garcia, H. Chiral Salen Complexes: An Overview to Recoverable and Reusable Homogeneous and Heterogeneous Catalysts. *Chem. Rev.* **2006**, *106*, 3987–4043. [[CrossRef](#)] [[PubMed](#)]
88. Akine, S.; Matsumoto, T.; Nabeshima, T. Spontaneous formation of a chiral supramolecular superhelix in the crystalline state using a single-stranded tetranuclear metallohelicate. *Chem. Commun.* **2008**, 4604–4606. [[CrossRef](#)] [[PubMed](#)]
89. Akine, S.; Hotate, S.; Matsumoto, T.; Nabeshima, T. Spontaneous enrichment of one-handed helices by dissolution of quasiracemic crystals of a tetranuclear single helical complex. *Chem. Commun.* **2011**, *47*, 2925–2927. [[CrossRef](#)] [[PubMed](#)]
90. Akine, S.; Nagumo, H.; Nabeshima, T. Hierarchical Helix of Helix in the Crystal: Formation of Variable-Pitch Helical  $\pi$ -Stacked Array of Single-Helical Dinuclear Metal Complexes. *Inorg. Chem.* **2012**, *51*, 5506–5508. [[CrossRef](#)] [[PubMed](#)]
91. Akine, S.; Matsumoto, T.; Nabeshima, T. Overcoming Statistical Complexity: Selective Coordination of Three Different Metal Ions to a Ligand with Three Different Coordination Sites. *Angew. Chem. Int. Ed.* **2016**, *55*, 960–964. [[CrossRef](#)] [[PubMed](#)]
92. Akine, S.; Hotate, S.; Nabeshima, T. A Molecular Leverage for Helicity Control and Helix Inversion. *J. Am. Chem. Soc.* **2011**, *133*, 13868–13871. [[CrossRef](#)] [[PubMed](#)]
93. Akine, S.; Miyashita, M.; Piao, S.; Nabeshima, T. Perfect encapsulation of a guanidinium ion in a helical trinickel(II) metallocryptand for efficient regulation of the helix inversion rate. *Inorg. Chem. Front.* **2014**, *1*, 53–57. [[CrossRef](#)]
94. Akine, S.; Miyashita, M.; Nabeshima, T. A Metallo-molecular Cage That Can Close the Apertures with Coordination Bonds. *J. Am. Chem. Soc.* **2017**, *139*, 4631–4634. [[CrossRef](#)] [[PubMed](#)]
95. Akine, S.; Shimada, T.; Nagumo, H.; Nabeshima, T. Highly cooperative double metalation of a bis(N<sub>2</sub>O<sub>2</sub>) ligand based on bipyridine-phenol framework driven by intramolecular  $\pi$ -stacking of square planar nickel(II) complex moieties. *Dalton Trans.* **2011**, *40*, 8507–8509. [[CrossRef](#)] [[PubMed](#)]
96. Akine, S.; Nagumo, H.; Nabeshima, T. Programmed multiple complexation for the creation of helical structures from acyclic phenol-bipyridine oligomer ligands. *Dalton Trans.* **2013**, *42*, 15974–15986. [[CrossRef](#)] [[PubMed](#)]
97. Akine, S.; Akimoto, A.; Nabeshima, T. Synthesis of Ag<sup>+</sup>-Selective Dipalladium(II) Metallohost Based on O-Alkyloxime Bis(N<sub>2</sub>SO) Ligands. *Phosphorus Sulfur Silicon Relat. Elem.* **2010**, *185*, 1000–1007. [[CrossRef](#)]
98. Akine, S.; Matsumoto, T.; Taniguchi, T.; Nabeshima, T. Synthesis, Structures, and Magnetic Properties of Tri- and Dinuclear Copper(II)–Gadolinium(III) Complexes of Linear Oligooxime Ligands. *Inorg. Chem.* **2005**, *44*, 3270–3274. [[CrossRef](#)] [[PubMed](#)]
99. Akine, S.; Kagiya, S.; Nabeshima, T. Oligometallic Template Strategy for Ring-Closing Olefin Metathesis: Highly Cis- and Trans-Selective Synthesis of a 32-Membered Macrocyclic Tetraoxime. *Inorg. Chem.* **2007**, *46*, 9525–9527. [[CrossRef](#)] [[PubMed](#)]
100. Akine, S.; Taniguchi, T.; Nabeshima, T. Acyclic Bis(N<sub>2</sub>O<sub>2</sub> chelate) Ligand for Trinuclear d-Block Homo- and Heterometal Complexes. *Inorg. Chem.* **2008**, *47*, 3255–3264. [[CrossRef](#)] [[PubMed](#)]
101. Akine, S.; Utsuno, F.; Nabeshima, T. Visible and Near-infrared Luminescence of Helical Zinc(II)–Lanthanide(III) Trinuclear Complexes Having Acyclic Bis(N<sub>2</sub>O<sub>2</sub>) Oxime Ligand. *IOP Conf. Ser. Mater. Sci. Eng.* **2009**, *1*, 012009. [[CrossRef](#)]

